Magnetic field decoupling and 3D-2D crossover in Nb/Cu multilayers

V. M. Krasnov
Institute of Solid State Physics, Russian Academy of Sciences, 142432 Chernogolovka, Russia and Physics Department, The Technical University of Denmark, DK-2800, Lyngby, Denmark

A. E. Kovalev and V. A. Oboznov
Institute of Solid State Physics, Russian Academy of Sciences, 142432 Chernogolovka, Russia

N. F. Pedersen
Physics Department, The Technical University of Denmark, DK-2800, Lyngby, Denmark

(Received 17 July 1996)

Transport properties of Nb/Cu multilayers were measured along and across layers. It is shown that not only the temperature but also the magnetic field parallel to layers can effectively decouple layers and cause the three-to-two–dimensional (3D-2D) crossover. As a consequence of the 3D-2D crossover, sharpening of the resistive transition with current along layers occurs due to the appearance of a strong intrinsic pinning in the 2D state. Evidence for the intrinsic Josephson effect in the 2D state is provided both by the periodic modulation of the dynamic resistance across layers versus the parallel magnetic field and by the multiply branched I-V curves caused by flux-flow of Josephson vortices in the stacked superconductor–normal-metal–superconductor junctions composing the multilayer. By measurements across layers the ''breaking field'' at which the proximity induced superconductivity in the normal layers of superconductor–normal-metal (Nb/Cu) multilayers is destroyed was observed directly. A dimensionality diagram in the (H-T) plane was deduced from our data. Reasons for complication of the ''Fraunhofer pattern,'' $I_c(H)$, in ''long'' multilayers are discussed. [S0163-1829(96)08046-0]

I. INTRODUCTION

Properties of superconducting multilayers (ML's) are of considerable interest both from the point of view of their application in cryoelectronics and from the general scientific point of view. It appears that multilayered structures have unique physical properties that are quite different from those of both bulk superconductors and thin films. These new properties could be advantageously used for fabrication of new cryoelectronic devices. Probably the first device of this type was a dc transformer by Giaever.[1] Among modern applications of ML structures we mention: (i) Flux-flow oscillators based on stacked Josephson junctions in which electromagnetic coupling of junctions changes the Swihart velocity,[2] and even more important, frequency multiplication could be possible due to generation of higher harmonics that occurs for different fluxon modes in the stack.[3] (ii) ML structures could be used in various superconducting particle detectors. For example, in the x-ray detector the trapping layer adjacent to the tunnel barrier is employed in order to reduce quasiparticle losses and thus increase the resolution of the detector.[4] (iii) The multilayered technology in general could provide a new level of integration in Josephson microelectronics. An example of that is a Josephson volt standard in which the introduction of stacks instead of series connected single junctions could decrease the size of the chip and improve the operation of the setup.[5] The necessary multifilm technology is already now used in single junction devices.

Superconducting ML's are also very interesting objects for fundamental science, exhibiting quite unusual physical phenomena. Those have been intensively studied in the last years especially in connection with high-T_c superconductors (HTSC) and organic superconductors. It is well known that HTSC have a layered structure with superconductivity mainly confined in the Cu-O layers and exhibit high anisotropy of physical properties. It especially concerns Tl and Bi based compounds that behave as layered superconductors in the sense that they exhibit quasi-two-dimensional properties. The dimensionality and the change of dimensionality, i.e., dimensional transitions, play a crucial role for the properties of such superconductors. For example the ''irreversibility line'' in the (H-T) plane (the magnetic field perpendicular to layers, $H\|c$) observed for various HTSC's could be satisfactorily explained by a three-to-two–dimensional (3D-2D) phase transition of the vortex lattice caused by the disintegration of the three-dimensional vortex line and the appearance of quasi-two-dimensional ''pancake'' vortices in individual layers.[6] The strong experimental evidence that Tl and Bi based HTSC's are layered superconductors is the observation of intrinsic Josephson effect between individual superconducting layers.[7,8] Another important question related to the layered structure of HTSC is what the properties of intermediate layers between copper-oxide layers are, i.e., whether they are superconducting, S', normal, N, insulating, I, etc. There exist some evidence that several HTSC compounds may have SNS structure.[8–11] For understanding of HTSC properties caused by its layered structure, experiments on model low-T_c ML with well defined parameters are of great importance. Artificial multilayers are convenient objects for this purpose since their characteristics could be controlled and varied over a wide range.

One of the peculiar properties of superconducting multi-

 © 1996 The American Physical Society

layers (ML's) is the three-to-two (3D-2D) dimensional crossover which consists of the fact that the ML behaves as being uniform across layers at $T>T_{2D}$ (3D state), while at lower temperatures individual layers are distinguishable and the ML is in the 2D state. The 3D-2D crossover was observed experimentally for various types of superconducting multilayers having different structures such as superconductor-insulator-superconductor (SIS), e.g., Pb/C,[12] superconductor-semiconductor-superconductor, e.g., Nb/Ge,[13] superconductor–normal-metal–superconductor (SNS), e.g., Nb/Cu,[14–16] V/Ag,[17] and V/Cu,[18,19] superconductor–magnetic-metal–superconductor (SMS), e.g., V/Ni,[20] and superconductor-superconductor′-superconductor (SS′S), e.g., Nb/NbTi,[21] and Nb/NbZr,[22] and some other. In all the mentioned cases, independent of the structure of the multilayers a linear-to-square root transition in the temperature dependence of the upper critical field parallel to layers, $H_{c2}^{\parallel}(T)$, was observed, representing the 3D-2D crossover.

Theoretically 3D-2D crossover was studied in several papers.[23–25] The important starting point for understanding of the 3D-2D crossover is given by the phenomenological Lawrence-Doniach (LD) model.[26] As it was shown by Lawrence and Doniach, properties of layered superconductors can be described by the three-dimensional anisotropic Ginzburg-Landau (GL) equations for disturbances that vary slowly with respect to the interlayer periodicity, s, in which case the ML is in the 3D state and behaves as a uniform across layers superconductor. The natural condition for the slow variation of the GL order parameter is that the coherence length in the direction across layers, $\xi_s^{\perp}$, should be greater than the interlayer spacing. The coherence length of the superconducting layer diverges as the temperature approaches T_c. Thus the multilayer is in a 3D state in the vicinity of T_c. With decreasing temperature $\xi_s^{\perp}$ decreases and the crossover from 3D to 2D state occurs when[23]

$$\xi_s^{\perp}(T_{2D})\sim s/\sqrt{2}. \tag{1}$$

At lower temperatures, $T<T_{2D}$, the layers become distinguishable for vortices since the size of the vortex core becomes less than s.

The 3D-2D crossover strongly influences major properties of the ML. One of the important consequences of the 3D-2D crossover is the appearance of Josephson properties in the 2D state, when layers are distinguishable and the ML can be considered as a stack of Josephson junctions. Thus in the 2D state intrinsic Josephson effect between individual layers of the ML exists.[27] Among the manifestations of the 3D-2D crossover we mention the following. (i) Linear-to-square root transition in $H_{c2}^{\parallel}(T)$.[12–22] As it follows from the LD model in the vicinity of T_c, the ML behaves as a 3D anisotropic superconductor with linear temperature dependence of $H_{c2}^{\parallel}$: $H_{c2}^{\parallel}(3D)\sim(1-T/T_c)$. However, with decreasing temperature the transition to the square-root temperature dependence occurs, $H_{c2}^{\parallel}(2D)\sim(1-T/T^*)^{1/2}$, which is typical for 2D superconducting films. Thus the upturn of $H_{c2}^{\parallel}(T)$ occurs. This is caused by the fact that in the 2D state vortex cores are situated between S layers and cannot destroy superconductivity in the S layers so that the pair function (condensation amplitude) in high magnetic fields is almost confined in the S layers.[24] (ii) Another manifestation is the change of the angular dependence of the upper critical field, $H_{c2}(\theta)$.[14,15] In the 3D state $H_{c2}(\theta)$ has a ''bell''-like shape with smooth variation at $\theta=0$ (parallel to layers), while in the 2D state $H_{c2}(\theta)$ has a ''cusp'' at $\theta=0$ typical for 2D superconducting films.[28] (iii) Steplike change of the anisotropy of the lower critical field, $\alpha=H_{c1}^{\perp}/H_{c1}^{\parallel}$, occurs at $T=T_{2D}$.[16] The sharp increase of the anisotropy at $T<T_{2D}$ is caused by decrease of the core energy for the vortex, parallel to layers, and thus by decrease of $H_{c1}^{\parallel}$, when the vortex core could be imbedded between S layers. (iv) An influence of the 3D-2D crossover on the critical current across layers, I_c, for Nb/Cu multilayers was observed in Ref. 25. In the 2D state, $T<T_{2D}$, the slope of the temperature dependence, $I_c(T)$, changes and follows the temperature dependence for an isolated Nb film, $I_c(2D)\sim\{1-T/T_c(\mathrm{Nb})\}$, while at higher temperatures $I_c(3D)\sim\{1-T/T_c(\mathrm{Nb/Cu})\}$. This is caused by the fact that in the 2D state the order parameter in S layers is close to its equilibrium value for the isolated superconductor. (v) Appearance of a hysteresis in the I-V curves (IVC's) with current applied across layers at $T=T_{2D}$ was observed for Nb/Cu multilayers in Refs. 25, 27. This is also evidence for the appearance of Josephson properties in multilayers in the 2D state. The hysteresis in the IVC's is an intrinsic property of a Josephson junction and is caused by the capacitance of the junction. With the crossover to the 2D state, Josephson junctions with a finite capacitance appear in the ML and causes the hysteresis in the IVC's. (vi) Recently the dramatic change in the characteristic magnetic length, Λ, of Josephson junctions and the corresponding change of the periodicity of Fraunhofer patterns of the critical current across layers, $I_c(H)$, in Nb/Cu multilayers was observed.[29] The period of oscillations is defined as $\Delta H=\Phi_0/L\Lambda$, where Φ_0 is a flux quantum and L is the longitudinal size of the junction. For T close to T_c the multilayers behave as a single SS′S junction (top Nb electrode–Nb/Cu ML–bottom Nb electrode) with the magnetic length $\Lambda_{3D}=D+2\lambda_{\mathrm{Nb}}$, where $D=Ns$ is the total thickness of the ML, N is the number of junctions in the ML, and λ_{Nb} is the penetration depth of Nb electrodes. On the other hand, in the 2D state, when the ML consists of stacks of Josephson junctions, $\Lambda_{2D}=s$.[30] In Ref. 29 the observed ratio, $\Lambda_{3D}/\Lambda_{2D}$, was more than twenty. (vii) Finally the 3D-2D crossover and the process of subdivision of the ML in individual layers was observed directly from the change of Josephson properties of Nb/Cu multilayers consisting of ten stacked Nb/Cu/Nb junctions.[27] The sequential increase of the voltage of the first Shapiro step in the IVC's was observed with decreasing temperature, representing the increase of the number of available and synchronized Josephson junctions in the ML. At temperatures close to T_c the voltage of the Shapiro step always obeyed the fundamental frequency-to-voltage relation, $V=\hbar\omega/2e$, so that multilayers behave as a single SS′S (top Nb electrode–Nb/Cu ML–bottom Nb electrode) junction, representing a pure 3D state. On the other hand, at low temperatures the Shapiro step was given by $V=10\hbar\omega/2e$, so that all ten Nb/Cu/Nb junctions were distinguishable and the ML's were in the 2D state.

The second crossover from the 2D to the 2D strongly coupled (2D-2DSC) state could take place in SNS (Ref. 31) and SS′S ML (Ref. 24) with further decrease of the temperature. In both cases the 2D-2DSC crossover is caused by the increase of the interlayer coupling. For SNS ML this is due to the temperature dependence of the coherence length of N

layers which causes the increase of the proximity effect with decreasing temperature.[31] In SS′S ML the effect is more trivial and is caused by the growth of superconductivity in S' layers at $T<T_c(S')$.

However, not only the temperature but also the magnetic field may influence the coupling between layers. An example is the already mentioned 3D-2D vortex lattice phase transition in layered superconductors[6] in a field perpendicular to layers. Yet it is not the coupling between layers itself but rather the coupling of the pancake vortices in the vortex line that is influenced by the perpendicular magnetic field. When the magnetic field is inclined with respect to layers in ML the vortex lattice transition from the straight to the kinked vortices could occur. Evidence of this type was probably observed in Refs. 32 and 33. The field parallel to layers on the other hand could effectively decouple layers via the phase fluctuations[34] or in the case of SNS ML due to destruction of the proximity induced superconductivity in N layers at a certain ''breaking field,'' $H_{\rm br}$.[35] For example, a typical three-to-two–dimensional transition in the angular dependence of the critical current of Nb/NbZr multilayers was observed with the change of magnetic field in Ref. 32.

In this paper the influence of the magnetic field on the coupling between layers in Nb/Cu ML's is studied. As it was mentioned previously[27] for direct measurements of the coupling between layers experiments with current applied across layers are necessary. Here we present results of resistive measurements with the current both along and across layers. When both the current and the magnetic field are parallel to layers ($I\perp H$) a sharpening of the resistive transition was observed at $T<T_{2D}$, which was explained by the appearance of an intrinsic pinning in the 2D state. By resistive measurements with the current across layers and the magnetic field parallel to layers we observed directly the magnetic field induced decoupling of layers and obtained the value of the breaking field. It was shown that the magnetic field parallel to layers effectively decouples layers in ML so that the 3D-2D crossover occurs when either the temperature is decreased below T_{2D} or when the magnetic field parallel to layers exceeds the ''breaking field,'' $H_{\rm br}$. The ML dimensionality diagram on the (H-T) plane was derived from our data. Periodic modulation of the dynamic resistance across layers versus the parallel magnetic field as well as multiply branched I-V curves caused by flux flow of Josephson vortices in the stacked SNS junctions composing the multilayer were observed and taken as evidence for the intrinsic Josephson effect in the 2D state. Reasons for complication of the Fraunhofer patterns in ''long'' ML's are discussed.

II. EXPERIMENT

Nb/Cu ML's were fabricated by rf sputter deposition and photolithography. For measurements along layers the sample had the form of a bridge consisting of 12 Nb layers and 13 Cu layers so that top and bottom layers were of Cu to avoid the problem related to surface superconductivity. For measurements across layers a special sample with a small cross section was fabricated in order to increase the sample resistance. In this case the sample consisted of 11 Nb layers (including Nb electrodes) and 10 Cu layers thus composing ten stacked SNS junctions. Previous measurements have shown that all the ten stacked junctions had identical properties.[27] Details of sample fabrication can be found elsewhere.[29,27] For resistive measurements we used a standard four probe scheme when the current was applied along layers and a superconducting two probe (no contact resistance) scheme for measurements across layers. The differential resistance, R_d, was measured by applying an ac current with a frequency of several hundred Hz and an amplitude 5–10 μA. The voltage was measured by a lock-in amplifier. For dc measurements of current-voltage characteristics the signal was filtered to decrease external noise. The sample was placed in a He exchange gas and the temperature was controlled by a temperature controller in the range 1–20 K. The magnetic field was provided by a superconducting coil and measured by a Hall sensor.

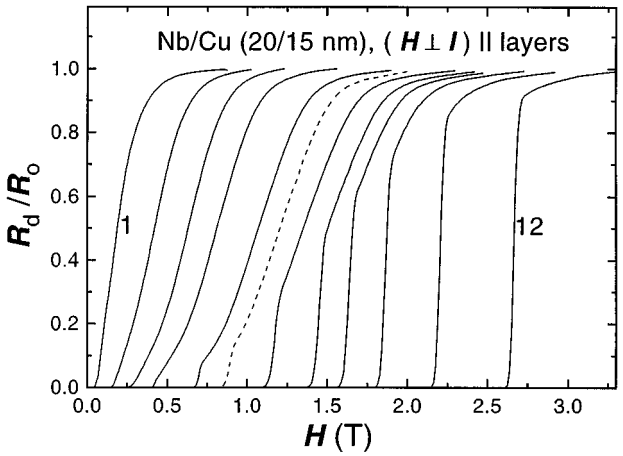

FIG. 1. Longitudinal resistive transitions $R_d(H)$ for Nb/Cu ML (20/15 nm) at constant temperature T=7.2, 6.8, 6.5, 6.2, 5.7, 5.5, 5.3, 5.0, 4.8, 4.6, 4.2, 3.7 (K) (curves 1–12, respectively) in parallel magnetic field ($I\perp H$). Sharpening of the transitions occurs at $T<T_{2D}\sim$5.5 K (dashed curve).

III. RESULTS AND DISCUSSION

A. Longitudinal measurements

In Fig. 1 resistive transitions $R_d(H)$ at constant temperature T=7.2, 6.8, 6.5, 6.2, 5.7, 5.5, 5.3, 5.0, 4.8, 4.6, 4.2, 3.7 (K) (curves 1–12, respectively) with both magnetic field and bias current parallel to layers ($I\perp H$) for Nb/Cu ML (20/15 nm) are shown (the experimental configuration in this case is shown schematically in Fig. 4). The characteristic feature of Fig. 1 is a sudden sharpening of transitions at $T<T^*\sim$5.5 K (dashed curve in Fig. 1). This is in contrast to the $R_d(H)$ behavior in a perpendicular magnetic field. In the latter case $R_d(H)$ curves are simply shifted to larger H with decreasing T without significant change of the transition width. This is illustrated in Fig. 2 where resistive transitions $R_d(H)$ for magnetic field perpendicular and the bias current parallel to layers are shown at constant temperature T=6.2, 5.7, 5.3, 5.0, 4.7, 4.5, 4.3, 4.0, 3.4, 3.0 (K) (curves 1–9, respectively) for Nb/Cu ML (20/20 nm). In Fig. 3 temperature dependencies of upper critical fields, $H_{c2}(T)$, obtained by 50% of the resistive transition, $R_d(H)$, are shown for Nb/Cu ML's (20/15 nm) and (20/20 nm) and for the magnetic field parallel (open symbols) and perpendicular (solid symbols) to lay-

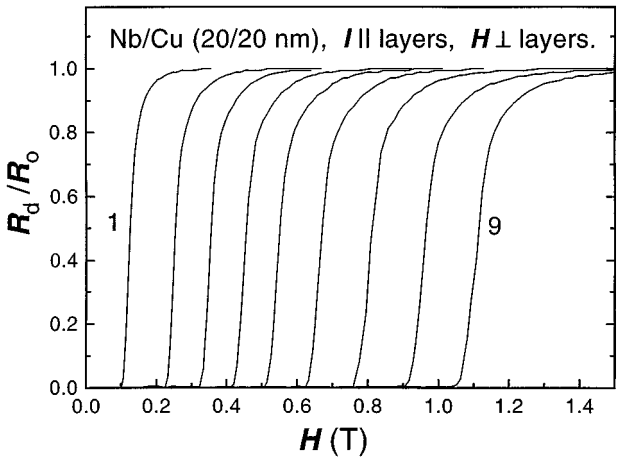

FIG. 2. Longitudinal resistive transitions $R_d(H)$ for Nb/Cu ML (20/20 nm) at constant temperature $T=6.2$, 5.7, 5.3, 5.0, 4.7, 4.5, 4.3, 4.0, 3.4, 3.0 (K) (curves 1–9, respectively) in a perpendicular magnetic field.

ers. The linear-to-square root transition representing the 3D-2D crossover is clearly seen on the $H_{c2}^{\parallel}(T)$ dependence for both samples. Solid and dashed lines in Fig. 3 represent the best square root fit to the $H_{c2}^{\parallel}(T)$ dependencies. No visible change in the behavior of the upper critical field perpendicular to layers was observed.

We identify the 3D-2D crossover temperature, T_{2D}, as the temperature at which the square root dependence (solid and dashed lines in Fig. 3) crosses the T axis ($H=0$) rather than the temperature at which the linear to square root transition in $H_{c2}^{\parallel}(T)$ occurs. We do so not only because the latter temperature is not well defined and moreover it depends on the criterion for determination of H_{c2} (see Fig. 9); however, the main reason is that, as seen from Fig. 1, the change in the properties of ML occurs at a temperature close to T_{2D} defined above, i.e., at a higher temperature than that defined by the linear-to-square root transition (Fig. 3). From Fig. 3 we obtain $T_c \cong 7.5$ K, $T_{2D} \cong 5.6$ K for the ML (20/15 nm) and

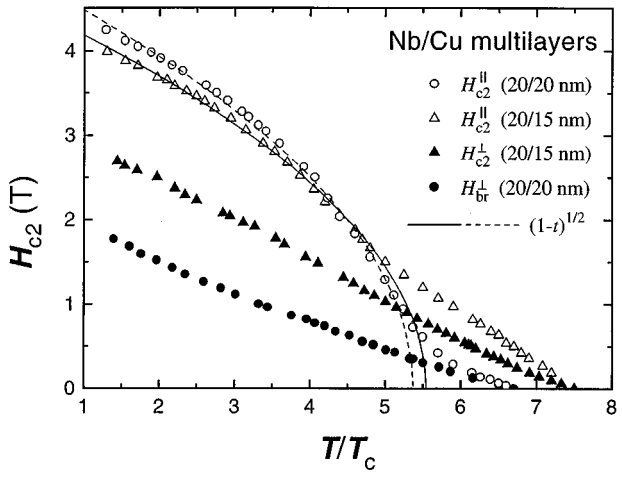

FIG. 3. Temperature dependencies of upper critical fields, $H_{c2}(T)$, obtained by 50% of the resistive transition, $R_d(H)$, for Nb/Cu ML (20/15 nm) and (20/20 nm) and for the magnetic field parallel (open symbols) and perpendicular (solid symbols) to layers. Solid and dashed lines represent the best square root fits.

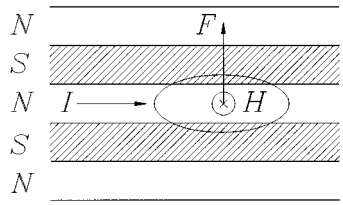

FIG. 4. The experimental configuration and the direction of the Lorentz force, F, acting on the vortex for longitudinal measurements in parallel magnetic field.

$T_c \cong 6.7$ K, $T_{2D} \cong 5.3$ K for the ML (20/20 nm). Thus both the critical temperature of the ML, T_c, and the crossover temperature, T_{2D}, decrease with increasing thickness of the N layers in qualitative agreement with calculations.[25]

The sharpening of the resistive transitions in a parallel magnetic field has been already observed for V/Cu ML's.[19] The authors explained the change in the transition width with decreasing temperature by a double dimensional transition: 3D-2D and 2D-3D (we would say 2D-2DSC). Their idea was supported by the observation of fluctuation paraconductivity of 3D type at high temperature, 2D type at intermediate temperatures, and again a 3D type at low temperature, and by the observation of the second upturn of $H_{c2}^{\parallel}(T)$ at low temperatures. Thus the width of the resistive transition was assumed to decrease at lower temperatures with transition of the ML into the 3D (2DSC) state.

Although the second 2D-2DSC crossover could take place in SNS ML with decreasing temperature due to the temperature dependence of the coherence length of N layers[31] such an explanation is unlikely in our case. First of all we do not observe any upturn of $H_{c2}^{\parallel}(T)$ at low temperatures for our Nb/Cu samples. On the contrary, as it can be seen from Fig. 3, the experimental $H_{c2}^{\parallel}(T)$ is even less than the square root dependence at low temperatures. Next, the 2D-2DSC crossover should occur at a temperature much lower than that corresponding to the appearance of sharpening of the resistive transition. Having studied the fluctuation paraconductivity behavior we did not observe any unusual change in dimensionality at low temperatures. We were able to observe only ordinary change in dimensionality of fluctuation paraconductivity predicted by the Lawrence-Doniach model[26] so that fluctuations had a clear 2D nature, $\Delta\sigma \tilde{} (1-T/T_c)^{-1}$, at T and H above T_c and H_{c2}, respectively, and 3D-like nature, $\Delta\sigma \tilde{} (1-T/T_c)^{-1/2}$, in the vicinity of T_c and H_{c2}. At T and H lower than T_c and H_{c2} paraconductivity did not follow neither 2D nor 3D behavior, which probably means that another mechanism of resistivity (e.g., flux flow) takes place. From Fig. 1 it is seen that sharpening of the resistive transition could occur well below the upper critical field (curves 5–7) where the fluctuations are not important. Thus we do observe the sharpening of the resistive transition, although it cannot be explained by fluctuations in our case.

All this brings us to an alternative interpretation of the sharpening of the resistive transition in parallel magnetic field. We start from the assumption that the voltage measured during the resistive transition has a flux-flow origin. In Fig. 4 the experimental configuration and the direction of the Lorentz force acting on the vortex is shown. The transport current along layers pushes vortices parallel to layers in the

direction across layers. When the ML is in the 3D state vortices can move freely across layers since the vortex dimensions are much larger than the interlayer spacing s. However, in the 2D state the vortex parallel to layers becomes of the Josephson type with the core imbedded in the N layer. Such a transition is accompanied by reduction of the fluxon energy.[16] Now to move the vortex across layers it is necessary to spend energy for formation of the normal core in the S layer. Then strong intrinsic pinning appears[36] preventing vortex motion across layers, which sharpens the resistive transition in parallel field. On the other hand, when the magnetic field is perpendicular to layers and the current is along layers the Lorentz force pushes vortices along layers. Taking into account that such motion does not change the fluxon energy it becomes clear why the 3D-2D crossover does not change the resistive transition in a perpendicular magnetic field; see Fig. 2. As is seen from Fig. 1 the sharpening of $R_d(H)$ is developed gradually with decreasing temperature from curve 4 to 12 so that the region with reduced transition width occupies sequentially a larger part of $R_d(H)$. This reflects the fact that the 3D-2D crossover itself is not sharp;[27] therefore the transition from ordinary to intrinsic pinning is not discontinuous so that the intrinsic pinning strengthens gradually with decreasing T below T_{2D}.

B. Transverse measurements

Longitudinal measurements could give only indirect information about the coupling between layers. On the other hand, measurements with current across layers do provide a crucial probe of the coupling. For measurements across layers special samples with small cross section (20 μm in diameter) were fabricated[29,27] (see the inset in Fig. 7). The resistive transition with I across layers should start first due to generation of Josephson voltage when the test current exceeds the critical current and finally should turn to the normal state resistance, in our case caused by the transition of the Cu layers into the normal state, when the parallel magnetic field exceeds $H_{\rm br}$. In Fig. 5 the transverse resistance ($I\perp$layers) behavior of Nb/Cu ML in parallel magnetic field is shown. The dashed line in Fig. 5 shows the $R_d(H)$ curve of Nb/Cu (20/15 nm) ML at $T=7.5$ K, $H\|$layers, and $I\perp$layers. As it is seen, the resistive transition is broad and has a long low resistance tail starting from small magnetic fields. This is due to the fact that our ML's are highly anisotropic, $\alpha=10-15$, and the lower critical field parallel to layers, $H_{c1}^{\|}$, is very small, of the order of few Oe.[16] In the transverse measurements the generated voltage is due to flux flow motion of Josephson-type vortices along layers. The pinning for such motion is very weak. To understand this we note that pinning in type-II superconductors is mainly caused by a local reduction of the vortex core energy at the pinning center. In SNS ML's with zero electron-phonon interaction in N layers, there is no condensation energy in N layers,[37] the core energy of the parallel vortex is caused by extra damping of superconductivity in S layers by the vortex in the N layer due to the proximity effect.[16] This energy decreases sharply with the transition of ML into the 2D state.[16] Thus a small value of $H_{c1}^{\|}$ and weak pinning of parallel vortices cause the existence of a low resistance tail on $R_d(H)$. At larger fields, when the breaking field is exceeded, the transverse resistance increases sharply (2.5–2.7 kOe in Fig. 5) due to destruction of superconductivity in N layers.

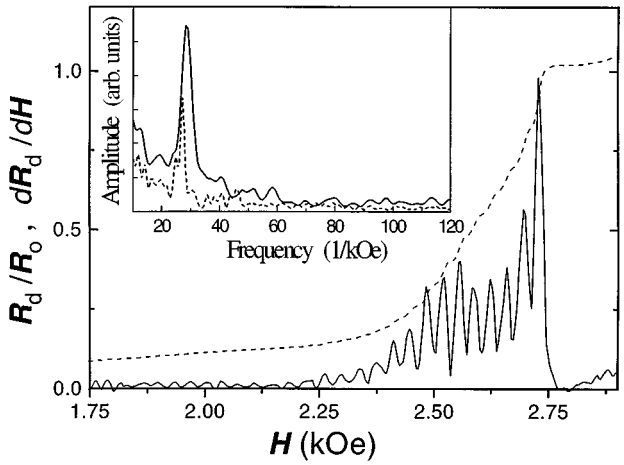

FIG. 5. A transverse resistive transition of Nb/Cu (20/15 nm) ML in parallel magnetic field (dashed line) at $T=7.5$ K. The solid curve represents the derivative $dR_d/dH(H)$; the Fourier spectrum of dR_d/dH is shown in the inset for two different field regions. Periodic oscillations of the transverse resistance as a function of magnetic field are obvious.

The solid curve in Fig. 5 represents the derivative $dR_d/dH(H)$; the Fourier spectrum of dR_d/dH is shown in the inset for two different field regions. Periodic oscillations of the transverse resistance as a function of magnetic field are obvious. These oscillations in our opinion are caused by the periodic ''Fraunhofer'' dependence $I_c(H)$ with each oscillation corresponding to the entrance of an additional flux quantum into the junction. The period $\Delta H\sim 30$ Oe perfectly coincides with that expected for a single intrinsic junction $\Delta H=\Phi_0/S$, where $S=L\Lambda$ is the quantization area with L the length of the junction, $L=20$ μm, and Λ the so-called ''magnetic length'' which for the intrinsic junction is simply equal to the interlayer periodicity of the ML,[30] $\Lambda=s=350$ Å. This means that the ML exhibits the intrinsic Josephson effect and hence is in the 2D state although for zero magnetic field $T=7.5$ K is deep inside the 3D region. Thus a parallel magnetic field can effectively decouple layers in superconducting ML.

At lower temperatures and at smaller resistances the oscillatory behavior of $R_d(H)$ was also observed; however, it was more complicated with some unstable switching, hysteresis, and without perfect periodicity. This is illustrated in Fig. 6, in which low resistance tails of $R_d(H)$ are shown for the same Nb/Cu (20/15 nm) ML as in Fig. 5 but for lower temperatures $T=6.2$, 5.6, 5.2, and 4.9 K. Such behavior is consistent with previous observations of a complicated Fraunhofer pattern, $I_c(H)$, in our Nb/Cu ML (Ref. 29) and in stacked Nb/AlO_x/Nb ML,[38] which is caused by different fluxon configurations with a different number of fluxons in the intrinsic junctions.[39]

We would like to note that this ''irregularity'' of the magnetic field oscillations caused by irregularity of fluxon entry into the junctions of the ML could be due not only to a spread in parameters of the junctions, but could as well be the general property of ''long'' ML's with dimensions along layers larger than the Josephson penetration depth. Let us

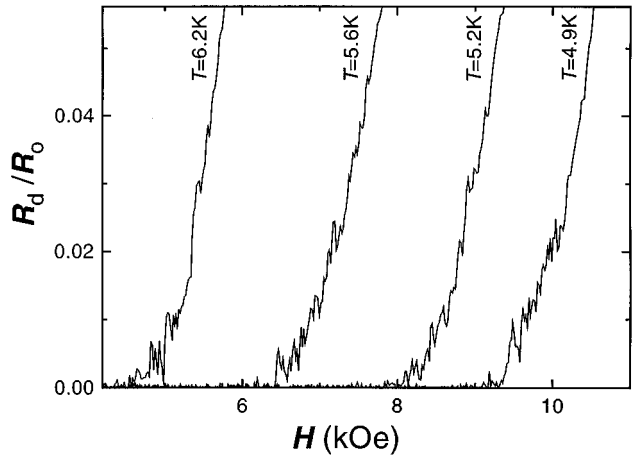

FIG. 6. Low resistance parts of transverse resistive transitions of Nb/Cu (20/15 nm) ML in parallel magnetic field at lower temperatures, $T=6.2$, 5.6, 5.2, and 4.9 K, when the ML is ''long.'' Complicated oscillatory behavior is seen.

consider a long ML consisting of N stacked junctions with length L and interlayer periodicity s. Fluxons will enter a single junction in average with periodicity

$$H_0(\mathrm{JJ})=\frac{\Phi_0}{Ls}. \tag{2}$$

On the other hand, fluxons will in average enter the ML with periodicity

$$H_0(\mathrm{ML})=\frac{\Phi_0}{LNs}, \tag{3}$$

in order not to have a big difference between the magnetic field intensity, H, and the magnetic field inductance, B, inside the ML. Otherwise large magnetization, $M=(B-H)/4\pi$, will appear in the ML. Equations (2) and (3) become exact at magnetic fields large compared to the lower critical field when the screening properties of the ML are weak.

At low magnetic field another problem exists, i.e., the difference in low critical fields of a single junction and the multilayer.[40] The lower critical field of the single intrinsic junction is equal to

$$H_{c1}(\mathrm{JJ})=\frac{2\Phi_0}{\pi^2\lambda_J s}, \tag{4}$$

while for the ML in parallel magnetic field it is[41]

$$H_{c1}^{\parallel}(\mathrm{ML})=\frac{\Phi_0}{4\pi\lambda_z\lambda_{xy}}\left[\ln\left(\frac{\lambda_z}{s}\right)+112\right]. \tag{5a}$$

Here λ_J is the Josephson penetration depth: λ_z and λ_{xy} are the penetration depths perpendicular and parallel to layers which for SNS ML are equal to[42]

$$\lambda_z^{-2}=\frac{ds}{s}\lambda_s^{-2}+\frac{d_N}{s}\lambda_N^{-2},$$

$$\lambda_{xy}^2=\frac{ds}{s}\lambda_s^2+\frac{d_N}{s}\lambda_N^2+\lambda_J^2.$$

Here d_S, d_N are thicknesses and λ_S, λ_N are the penetration depths of S and N layers, respectively. Assuming that $\lambda_J\gg\lambda_N\gg\lambda_S$ we obtain

$$H_{c1}^{\parallel}(\mathrm{ML})\sim a\,\frac{\Phi_0}{4\pi\lambda_z\lambda_J}, \tag{5b}$$

where a is a constant of the order of unity. From comparison of Eqs. (2) and (3) and (4) and (5b) it is seen that for a thin layered ML, $N\gg1$, $s\ll\lambda_S$,

$$H_0(\mathrm{JJ})\gg H_0(\mathrm{ML}), \tag{6a}$$

$$H_{c1}(\mathrm{JJ})\gg H_{c1}^{\parallel}(\mathrm{ML}). \tag{6b}$$

Thus from Eqs. (6a) and (6b) it is seen that in the whole range of magnetic fields fluxons will not enter simultaneously all the junctions in the long ML. The IVC of the ML provides an integral characteristic of all the junctions in the ML and the critical current reduces each time when an additional fluxon enters one of the junctions in the ML. Thus in general different average periodicity in magnetic field could be observed from H_0(ML), Eq. (3), for absolutely irregular fluxon entrance to H_0(JJ), Eq. (2), for simultaneous fluxon entrance in all junctions.

For ''small'' ML's, $L<\lambda_J$, there is no such problem since there are no vortices in this case. The magnetic field is not screened by the small ML and the flux in all the intrinsic junctions will change simultaneously proportional to H. In this case perfect periodicity with the period H_0(JJ), Eq. (2), should be observed as that in Fig. 5.

Oscillations of $R_d(H)$ similar to those in Fig. 6 were observed also in HTSC (Ref. 43) and were related to the existence of intrinsic Josephson junctions between different CuO_2 layers. Oscillations of the critical current in the c direction, $I_c(H)$, for HTSC were observed in Refs. 7, 39, and 44. However, one should be careful estimating the interlayer periodicity, s, from not clearly periodic characteristics. As we discussed above occasional or regular switching between different fluxon modes in ML could cause extra modulation of $R_d(H)$ and $I_c(H)$ dependencies so that the interlayer periodicity could be systematically overestimated. This can be seen from Fig. 6 and it might be one of the reasons for getting smaller ''periodicity'' in magnetic field and larger s values in Refs. 43 and 44. Another common feature of our experiment on low-T_c ML and that of HTSC (Ref. 43) is that the oscillations are better defined at higher temperatures. The reason probably lies in the temperature dependence of the Josephson and the London penetration depths and of the coherence length. All of those diverge with approaching T_c. Due to the temperature dependence of the Josephson penetration depth, λ_J, the junction length may become larger than λ_J with decreasing temperature. Our estimation [$\lambda_J(T=0)\sim5$ μm (Ref. 16)] shows that for our ML's this happens at $T\sim0.2$–0.3 K below T_c. At lower temperatures the junctions in the ML become long and hysteresis due to fluxon pinning at the junction boundary as well as a possibility of different fluxon configurations in the ML contribute to complication of the $R_d(H)$ oscillations. The temperature

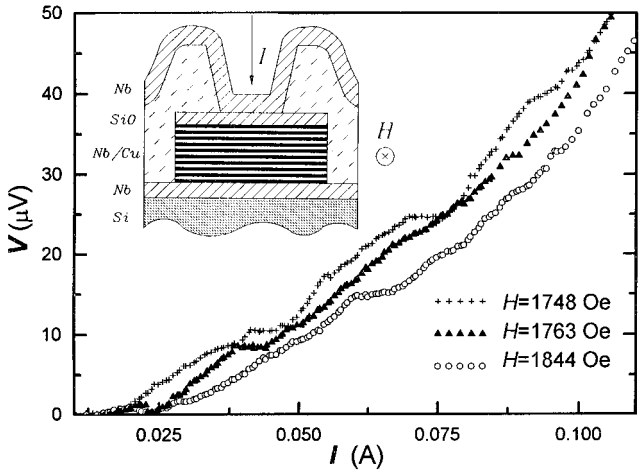

FIG. 7. Transverse I-V curves for Nb/Cu (20/15 nm) ML in parallel magnetic field, $H=1748$, 1763, and 1844 Oe, and at $T=4.2$ K. The existence of steps with constant voltage is seen. In the inset the sketch of the sample and the experimental configuration are shown.

dependence of the London penetration depths and the coherence length result in stronger inductive and quasiparticle coupling of fluxons in stacked junctions at higher temperatures, strengthening the synchronization of the junctions of the ML.

Different fluxon modes in the ML are better observed from the I-V curves. In Fig. 7 IVC's across layers of the same Nb/Cu (20/15 nm) ML are shown for three different values of the applied parallel magnetic field at $T=4.2$ K (the current 0.1 A corresponds to the current density 8×10^3 A/cm^2). In the inset the sketch of the sample and the experimental configuration are shown. From Fig. 7 it is seen that IVC's exhibit well defined steps with constant voltage. In general the behavior of IVC in a magnetic field was complicated with hysteresis for increasing and decreasing bias current (not shown). The characteristic feature of the IVC was the existence of multiple but distinct branches and switching between those branches while sweeping the current and magnetic field. This is illustrated in Fig. 8 in which a set of IVC's at constant temperature, $T=4.2$ K, and different parallel magnetic fields in the range 1.5–2.0 kOe is shown. Different symbols represent IVC's measured in different runs. The existence of distinct branches can be seen. On sweeping the current, the IVC was following one of the branches and could occasionally switch to the neighboring one. Thus sweeping the current up and down at the same magnetic field it was possible to draw several branches that were repeatedly reproduced. Changing the magnetic field did not change the branches but only changes a set of visible branches. Most of the IVC branches in Fig. 8 contain parts repeatedly drawn at different magnetic fields.

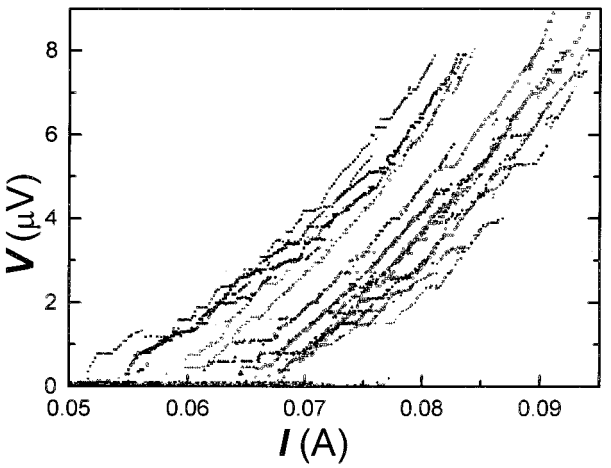

FIG. 8. A set of IVC's at $T=4.2$ K and different parallel magnetic fields in the range 1.5–2.0 kOe. Each run is represented by a particular symbol. The existence of multiple branches and step structure on IVC's is seen.

Multiple branches on the IVC were observed previously both for low-T_c SIS (Nb/AlO$_x$/Nb) ML (Refs. 5, 38, and 39) and for intrinsic HTSC junctions.[7,8,39] Those were attributed to the switching of additional junctions into the resistive state and thus the total number of possible branches was equal to the number of junctions in the stack. This is however definitely not the case for our ML's. The number of observed branches, even those shown in Fig. 8, exceeds ten–the number of junctions in the ML.

To our opinion the observed branches on IVC have a flux-flow nature and correspond to different fluxon modes in the ML, i.e., different number of fluxons in the junctions. Each time an additional fluxon leaves/enters one of the junctions the total IVC of the ML is switched to the other branch with lower/higher voltage. The horizontal steps with constant voltage on the IVC's most probably correspond to the synchronized motion of fluxons in all the junctions of the ML. Previously we have observed synchronization in the same samples caused by a small applied rf power.[27] The well defined synchronization phenomenon in our ML's is enabled due to small thicknesses of the layers (~15–20 nm) so that both inductive (interaction of fluxons in different junctions) and quasiparticle (quasiparticle current flow through the whole ML) synchronization are strong. We note that in our SNS ML's quasiparticle mechanism of synchronization could be the most important one. From Fig. 8 it can be seen that these horizontal steps on IVC's often have the same voltage for different branches. We can even argue that there is a fine step structure periodic in voltage on IVC's that might be caused by some kind of geometric resonances.

C. Dimensionality diagram

We can identify the field at which half of transverse resistive transition occurs, dashed curve in Fig. 5, as a breaking field, $H_{\rm br}(50\%)$. In Fig. 9 the obtained values of $H_{\rm br}(50\%)$ along with the values of the upper critical fields extracted from our longitudinal measurements are shown. Here $H_{c2}^{\parallel}$ and $H_{c2}^{\perp}$ (50%,90%) are the upper critical fields for $I\parallel$ layers and $H\parallel$ and $\perp$ to layers respectively determined from 50% and 90% of the resistive transition, see Figs. 1 and 2. The dashed line in Fig. 9 represents the best square root fit to $H_{c2}^{\parallel}$ in the 2D state. The difference $H_{c2}(90\%)-H_{c2}(50\%)$ reflects the width of the resistive transition. It is seen that for the perpendicular field there is no significant change in the transition width with decreasing T as shown in Fig. 2, while

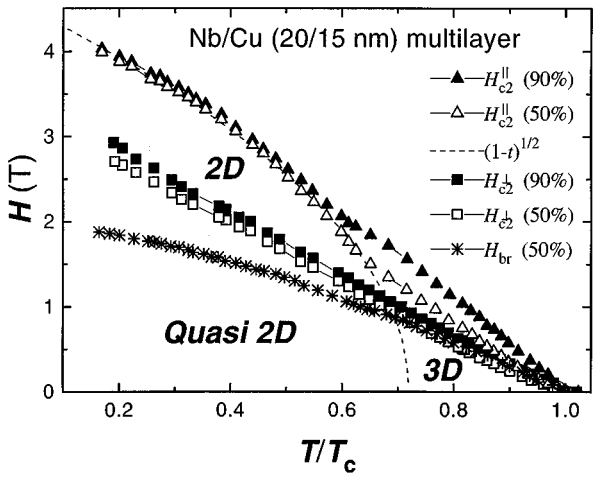

FIG. 9. Dimensionality (H-T) diagram for Nb/Cu (20/15 nm) ML. Temperature dependencies of the upper critical field and the breaking field are shown. The ML is in the 3D state in a region of small magnetic fields, $H<H_{\rm br}(T)$ and high temperatures, $T>T_{\rm 2D}$. At low temperatures, $T<T_{\rm 2D}$, and low magnetic fields, $H<H_{\rm br}(T)$, the ML is in a quasi-2D state and consists of Josephson coupled layers. At higher magnetic fields, $H_{c2}^{\parallel}(T)>H>H_{\rm br}(T)$, the ML is in the pure 2D state and consists of totally decoupled S layers.

for the parallel magnetic field sharpening of the transition occurs at $T<T_{\rm 2D}$ (see Fig. 1).

From Fig. 9 it is seen that for high temperatures, $T_c>T>T_{\rm 2D}$, the breaking field and the upper critical field $H_{c2}^{\parallel}$ are close to each other. This is not surprising since the coupling here is strong and breaking of superconductivity in N layers causes nearly simultaneous breaking in S layers. On the other hand, at $T<T_{\rm 2D}$ the difference between $H_{\rm br}$ and $H_{c2}^{\parallel}$ is well defined. This is due to the fact that the coupling here is weak and breaking of superconductivity in N layers cannot totally kill superconductivity in S layers. At fields $H_{c2}^{\parallel}>H^{\parallel}>H_{\rm br}$, the ML consist of a stack of decoupled S layers without superconductivity in the direction across layers since the proximity induced superconductivity in N layers is destroyed; however, the ML is still superconducting for the current along layers up to the field $H_{c2}^{\parallel}$ of the individual S layer, which naturally has the square root temperature dependence shown by the dashed line in Fig. 9. This brings us to a very simple explanation of the square root dependence of $H_{c2}^{\parallel}(T)$ in the 2D state. The temperature $T_{\rm 2D}$ obtained from the intersection of the square root dependence with the T axis ($H=0$) simply represents the critical temperature, $T_{\rm 2D}=T_c'(S)$, of the individual S layer surrounded by a pure normal metal with zero superconducting order parameter.

Thus we obtain the following dimensionality diagram of superconducting ML as a function of temperature and parallel magnetic field (see Fig. 9). The 3D state exists in a region of small magnetic fields, $H<H_{\rm br}(T)$ and high temperatures, $T>T_{\rm 2D}$. At low temperatures, $T<T_{\rm 2D}$, the layers in the ML become distinguishable and the ML transits into the 2D state. Here we can identify two different regions as a function of magnetic field. (i) At low magnetic fields, $H<H_{\rm br}(T)$, the ML is in a quasi-2D state and consists of Josephson coupled layers. (ii) At higher magnetic fields, $H_{c2}^{\parallel}(T)>H>H_{\rm br}(T)$, the ML is in the pure 2D state and consists of totally decoupled S layers.

IV. CONCLUSIONS

In conclusion we have shown that the magnetic field parallel to layers of superconducting ML effectively decouples layers and can cause the dimensional 3D-2D transition. By transport measurements across layers we directly obtained the breaking field at which proximity induced superconductivity in N layers of SNS (Nb/Cu) ML is destroyed and observed the transition of the ML to the 2D state with increasing the parallel magnetic field.

As evidence of magnetic decoupling of layers and the 3D-2D crossover we observed the following. (i) Sharpening of longitudinal resistive transition in a parallel magnetic field ($I\perp H$) at $T<T_{\rm 2D}$ which was explained by the appearance of an intrinsic pinning in the 2D state. (ii) Perfect periodic modulation of the dynamic resistance across layers versus the parallel magnetic field was observed for each period corresponding to the entrance of an additional flux quantum in the intrinsic junctions of the ML. (iii) Multiple branches on the IVC's across layers, attributed to flux flow of Josephson vortices in the stacked junctions, were observed, each corresponding to a particular fluxon mode in the ML.

Observation of a dc Josephson effect is an important confirmation of the Josephson nature of the coupling between layers in HTSC and other layered superconductors. The dc Josephson effect should in particular give rise to periodic oscillations of the critical current across layers and the resistivity versus the parallel magnetic field. Although qualitatively such oscillations were observed both for HTSC (Refs. 7, 39, 43, and 44) and low-T_c ML,[29,38,39] they were typically weak and very complicated, without clear periodicity, which finally resulted in a ''wrong'' value of the interlayer periodicity, s, of the layered structure. Oscillatory behavior in ML with perfect periodicity in H giving the exact value of s was observed here. General reasons for complication of the Fraunhofer pattern in ''long'' ML, $L>\lambda_J$, leading to overestimation of the interlayer periodicity were discussed. There are two possibilities to avoid this problem: (i) In-plane dimensions of the structure should be made smaller than the Josephson penetration depth and (ii) measurements at high temperatures, $T\sim T_c$, where $\lambda_J(T)>L$ should be performed. It might be also interesting to understand the dynamics of fluxon penetration into the layered superconductor with the change of the parallel magnetic field. We believe that some preferable fluxon modes (e.g., a flux lattice) should exist, which could make the fluxon entrance regular even for long ML's. Some evidence of this type was observed experimentally in Ref. 45.

ACKNOWLEDGMENTS

The work was supported in part by the Russian Foundation for Fundamental Research under the Grant No. 96-02-19319. One of us (V.M.K.) is grateful to the Technical University of Denmark for hospitality.

[1] I. Giaever, Phys. Rev. Lett. **15**, 825 (1965).
[2] A. V. Ustinov, M. Cirillo, H. Kohlstedt, G. Hallmanns, C. Heiden, and N. F. Pedersen, Phys. Rev. B **48**, 10 614 (1993).
[3] S. Sakai, A. V. Ustinov, H. Kohlstedt, A. Petraglia, and N. F. Pedersen, Phys. Rev. B **50**, 12 905 (1994).
[4] A. A. Golubov, E. P. Houwman, J. G. Gijsbertsen, V. M. Krasnov, M. Yu. Kupriyanov, J. Flokstra, and H. Rogalla, Phys. Rev. B **51**, 1073 (1995).
[5] A. Klushin, H. Kohlstedt, and G. Hallmanns, in *Proceedings of the EUCAS Conference*, edited by H. C. Freyhardt, Applied Superconductivity (DGM, Oberursel, 1993), p. 1261; A. M. Klushin and H. Kohlstedt, J. Appl. Phys. **77**, 441 (1995).
[6] M. V. Feigelman, V. B. Geshkenbein, and A. I. Larkin, Physica C **167**, 177 (1990); L. I. Glazman and A. E. Koshelev, Phys. Rev. B **43**, 2835 (1991).
[7] R. Kleiner, F. Steinmeyer, G. Kunkel, and P. Mueller, Phys. Rev. Lett. **68**, 2394 (1992); R. Kleiner and P. Mueller, Phys Rev. B **49**, 1327 (1994).
[8] A. Yurgens, D. Winkler, N. V. Zavaritsky, and T. Claeson, Phys. Rev. B **53**, R8887 (1996).
[9] V. M. Krasnov, Physica C **190**, 357 (1992).
[10] A. A. Golubov and V. M. Krasnov, Physica C **196**, 177 (1992).
[11] S. H. Liu and R. A. Klemm, Physica C **216**, 293 (1993).
[12] J. P. Locquet, D. Neerink, and H. Van der Straaten, Jpn. J. Appl. Phys. **26**, 1431 (1987).
[13] S. T. Ruggiero, T. W. Barbee, and M. R. Beasley, Phys. Rev. B **26** 4894 (1982).
[14] C. S. L. Chun, G. Zheng, J. L. Vicent, and I. K. Schuller, Phys. Rev. B **30**, 4915 (1984).
[15] I. Banerjee and I. K. Schuller, J. Low Temp. Phys. **54**, 501 (1984).
[16] V. M. Krasnov, A. E. Kovalev, V. A. Oboznov, and V. V. Ryazanov, Physica C **215**, 265 (1993).
[17] K. Kanoda, H. Mazaki, T. Yamada, H. Hosoito, and T. Shinjo, Phys. Rev. B **33**, 2052 (1986).
[18] V. I. Dedyu, V. A. Oboznov, V. V. Ryazanov, A. G. Sandler, and A. S. Sidorenko, Pis'ma Zh. Eksp. Teor. Fiz. **49**, 618 (1989) [JETP Lett. **49**, 712 (1989)].
[19] V. I. Dedyu, V. V. Kabanov, and A. S. Sidorenko, Phys. Rev. B **49**, 4027 (1994).
[20] H. Homma, C. S. L. Chun, G. Zheng, and I. Schuller, Phys. Rev. B **33**, 3562 (1986).
[21] M. G. Karkut, V. Matijasevic, L. Antognazza, J. M. Triscone, N. Missert, M. R. Beasley, and O. Fischer, Phys. Rev. Lett. **60**, 1751 (1988).
[22] Y. Kuwasawa, U. Hayano, T. Tosaka, S. Nakano, and S. Matuda, Physica C **165**, 173 (1990).
[23] R. A. Klemm, A. Luther, and M. R. Beasley, Phys. Rev. B **12**, 877 (1975).
[24] S. Takahashi and M. Tachiki, Phys. Rev. B **33**, 4620 (1986); **34**, 3162 (1986).
[25] V. M. Krasnov, N. F. Pedersen, and V. A. Oboznov, Phys. Rev. B **50**, 1106 (1994).
[26] W. E. Lawrence and S. Doniach, in *Proceedings of the 12th International Conference on Low Temperature Physics, Kyoto, 1970*, edited by E. Kanda (Academic, Kyoto, 1971), p. 361.
[27] V. M. Krasnov, N. F. Pedersen, V. A. Oboznov, and V. V. Ryazanov, Phys. Rev. B **49**, 12 969 (1994).
[28] M. Tinkham, Phys. Rev. **129**, 2413 (1963).
[29] V. M. Krasnov, V. A. Oboznov, V. V. Ryazanov, and N. F. Pedersen, *Proceedings of the International Workshop on Advanced Technology of Multicompositional Solid Films and Structures* (Dubrinich, Ukraine, 1994), pp. 35 and 36.
[30] L. N. Bulaevskii, J. R. Clem, and L. I. Glazman, Phys. Rev. B **46**, 350 (1992).
[31] V. M. Krasnov, Physica C **252**, 319 (1995).
[32] Y. Kuwasawa, T. Tosaka, A. Uchiyama, S. Matuda, and S. Nakano, Physica C **175**, 187 (1991); T. Nojima, M. Kinoshita, S. Nakano, and Y. Kuwasawa, *ibid*. **206**, 387 (1993).
[33] P. Koorevaar, W. Maj, P. H. Kes, and J. Aarts, Phys. Rev. B **47**, 934 (1993).
[34] K. B. Efetov, Zh. Exp. Teor. Fiz. **76**, 1781 (1979) [Sov. Phys. JETP **49**, 905 (1979)].
[35] G. Deutscher and P. G. de Gennes, in *Superconductivity II*, edited by R. D. Parks (Dekker, New York, 1969), pp. 1005–1034
[36] M. Tachiki and S. Takahashi, Solid State Commun. **70**, 291 (1989).
[37] There might be some core energy in N layers caused by the existence of Andreev levels. However, this energy is small and could be neglected in the first approximation.
[38] H. Amin, M. G. Blamire, and J. E. Evetts, IEEE Trans. Appl. Supercond. **3**, 2204 (1993); H. Kohlstedt, G. Hallmanns, I. P. Nevirkovets, D. Guggi, and C. Heiden, *ibid*. **3**, 2197 (1993).
[39] R. Kleiner, P. Mueller, H. Kohlstedt, N. F. Pedersen, and S. Sakai, Phys. Rev. B **50**, 3942 (1994).
[40] M. V. Fistul and G. F. Giuliani, Physica C **230**, 9 (1994).
[41] J. R. Clem, M. W. Coffey, and Z. Hao, Phys. Rev. B **44**, 2732 (1991).
[42] V. M. Krasnov, N. F. Pedersen, and A. A. Golubov, Physica C **209**, 579 (1993).
[43] D. C. Ling, G. Yong, J. T. Chen, and L. E. Wenger, Phys. Rev. Lett. **75**, 2011 (1995).
[44] Yu. I. Latyshev and J. E. Nevelskaya, Physica C **235–240**, 2991 (1994).
[45] M. Ziese, P. Esquinazi, P. Wagner, H. Adrian, S. H. Brongersma, and R. Griessen, Phys. Rev. B **53**, 8658 (1996).